Journal of Cultural Heritage 80 (2026) 26–35

Contents lists available at ScienceDirect

Journal of Cultural Heritage

journal homepage: www.elsevier.com/locate/culher

VSI: TECHNART 2025

# Protective coatings for outdoor bronze: Influence of application methodology on performance

Giulia Pellis[a,*], María Teresa Molina[b,c], Blanca Ramirez Barat[b], Emilio Cano[b], Paola Letardi[d], Barbara Salvadori[e], Caterina Biondi[e], Maxim Tiburziano[f], Barbara Giussani[g], Dominique Scalarone[a]

[a] Department of Chemistry, University of Torino, Via Pietro Giuria 7, Torino, Italy
[b] National Centre for Metallurgical Research (CENIM), Spanish National Research Council (CSIC), Avenida de Gregorio del Amo 8, 28040 Madrid, Spain
[c] Institute of Geosciences (IGEO), Spanish National Research Council (CSIC) and University Complutense of Madrid (UCM), Calle Dr. Severo Ochoa 7, 28040 Madrid, Spain
[d] Institute of Anthropic Impacts and Sustainability in marine environment (IAS), National Research Council (CNR), Via De Marini 6, 16123 Genoa, Italy
[e] Institute of Heritage Science (ISPC), National Research Council (CNR), Via Madonna Del Piano 10, 50019 Sesto Fiorentino, Italy
[f] CiQUS - Center for Research in Biological Chemistry and Molecular Materials, University of Santiago de Compostela, Calle Jenaro de la Fuente, Campus Vida, Santiago de Compostela, Spain
[g] Science and High Technology Department, Università degli Studi dell'Insubria, Via Valleggio 9, Como, Italy

ARTICLE INFO

*Article history:*
Received 15 November 2025
Accepted 28 April 2026

*Keywords:*
Acrylic coatings
Patinated bronze
Electrochemical measurements
Application method

ABSTRACT

Research on sustainable protective coatings for metallic heritage presents significant challenges due to the inherent complexity of corrosion processes in bronze, patina, and outdoor environmental systems. Additionally, the absence of standardised testing and evaluation methods hampers the comparability of results and the establishment of best practices. New sustainable coatings based on Paraloid® B44, with a light stabiliser and a corrosion inhibitor, have been optimised for a low toxicity profile. The tested formulations include Tinuvin® 312 as light stabiliser and 5-mercapto-1-pheniltetrazole (MPT) or 2-amino-5-ethyl-1,3,4-thiadiazol- (AEDTA) as corrosion inhibitors. Their physicochemical properties have been determined through multi-analytical characterisation and monitoring of changes during artificial solar light ageing. Nonetheless, the effectiveness of a coating is also greatly affected by the application method and the chemical, physical and morphological properties of the underlying surface. In this work, the role of Paraloid® concentration in a two-layer brush application method is addressed on quaternary bronze with a *Verde Messina* foundry patina. The influence of resin concentration on the resulting layer is analysed. Patinated bronze mock-ups were non-destructively characterised before and after treatment by Electrochemical Impedance Spectroscopy (EIS) to assess corrosion resistance, colour by colourimetry to evaluate visual appearance, and by Eddy Current to measure the patina and coating thickness. After artificial thermo-hygrometric ageing of the coated mock-ups, Fourier Transform Infrared Spectroscopy in external reflection mode (ER-FTIR) and colourimetry were used to assess the treatment stability with respect to molecular composition and colour changes. Principal Component Analysis (PCA) of ER-FTIR spectra allowed highlighting differences in coatings over the ageing process. Results showed that all tested treatments increased the corrosion resistance of Verde Messina patinated bronze; double-layer coatings with a more diluted first layer were found to be the preferred treatment, providing comparable performance while using a smaller amount of Paraloid®.



## 1. Introduction

Outdoor bronze objects are continuously exposed to both natural and anthropogenic degradation agents, which compromise their visual integrity and structural stability. Over time, these surfaces develop a layer of corrosion products known as patina, whose composition is strongly influenced by surface morphology, roughness, alloy composition, and environmental exposure conditions [1–3]. Patinas are valued not only for their aesthetic and historical significance but also for the degree of protection they provide to the underlying metal. However, this protective function

* Corresponding author.
*E-mail address:* giulia.pellis@unito.it (G. Pellis).

https://doi.org/10.1016/j.culher.2026.04.016

is often inadequate under polluted conditions, thus necessitating additional conservation measures [4]. Standard conservation practices aim to preserve the original appearance and material integrity of bronze artefacts by applying protective coatings that limit the interaction between environmental corrosive agents and the metal-patina interface [5]. Among the most widely employed protective treatments are polymer coatings, typically acrylic resins, and waxes. These coatings sometimes include additives such as benzotriazole (BTA), a compound found in the commercial product Incralac, which serves as an ultraviolet (UV) adsorber and corrosion inhibitor [6,7]. Despite its proven efficacy, BTA raises significant concerns due to its suspected toxicity and limited durability on treated surfaces, posing health and environmental risks [8,9]. In response to these concerns, recent research has focused on more eco-friendly alternatives, such as organosilanes, carboxylates, and fluoropolymers [10]. One innovative strategy has been the encapsulation of BTA within naturally derived nanocarriers, such as halloysite nanotubes or $\beta$-cyclodextrins, which offers improved stability and reduced toxicity while maintaining protective performance [11–13]. Regardless of the specific formulation, protective coatings for cultural heritage objects must meet stringent criteria, including transparency, reversibility, long-term stability, and compatibility with existing patinas [5,14].

However, evaluating such coatings remains a methodological challenge due to the absence of standardised testing protocols and the intrinsic variability of heritage surfaces. The variability and complexity of patinated substrates, in terms of their structural, chemical, and morphological characteristics, have been documented [15] and are expected to influence the behaviour of protective coatings on bare metals, artificially patinated surfaces, and naturally corroded substrates. In this context, a distinction should be made between the main categories of patinas considered in the study of copper-alloy corrosion and conservation treatments, namely naturally developed outdoor patinas, laboratory-produced artificial patinas, and foundry-applied artistic patinas. Natural outdoor patinas form over extended exposure periods under atmospheric conditions and typically develop a complex multilayered structure, often showing heterogeneity in stratigraphy, porosity, and mineralogical composition [16–19]. Laboratory-produced artificial patinas, on the other hand, are generated under controlled experimental conditions to reproduce selected chemical or structural features of naturally aged layers, providing reproducible substrates for mechanistic studies and protective treatments evaluation [3,15,20]. Foundry-applied patinas, such as the widely used “Verde Messina”, are created by artists and foundry practitioners to achieve specific colors and surface finishes on bronze artworks. While they do not reproduce the full complexity of naturally developed outdoor corrosion, they represent surfaces commonly encountered in artistic and conservation practice [3,18,21,22]. Therefore, the development of representative test samples, or mock-ups, that replicate the morphological and chemical complexity of heritage patinas is essential for meaningful evaluation [23]. In our previous studies, we primarily focused on the physical, optical, and mechanical properties of protective polymer films based on Paraloid® B44, with corrosion inhibitors and light stabilisers, with some preliminary evaluations conducted on bare bronze substrates [24–26]. These investigations allowed us to identify the most promising formulations in terms of stability, inhibitor retention, and UV resistance. However, as the interaction between a coating and a patinated surface is expected to influence its long-term performance significantly, further research was necessary to validate these formulations under more representative conditions.

Accordingly, the present study investigates the performance of the newly developed Paraloid® B44-based coatings applied to bronze mock-ups with foundry patina “Verde Messina”. This patina was selected as a practice-oriented substrate due to its use by artistic foundry and because other study already exist on nitrate type patina on artworks [3,4,21], pointing out its low protectiveness [3,4]. Consequently, the results should be interpreted specifically within the context of artistic and foundry patinas, rather than as direct analogues of long-term natural outdoor patinas.

This study represents an important step toward bridging the gap between polymer characterisation and practical application on artworks. In particular, the influence of resin concentration on the protective properties of a two-layer brush-applied system is investigated. Key parameters such as resin concentration, number of layers, and drying time between applications can significantly affect coating thickness, substrate penetration, coating film continuity and adhesion, ultimately influencing the efficacy and durability of the protective system [14]. These parameters, however, are difficult to assess on patinated samples due to inherent surface inhomogeneities. To address these challenges, this work proposes a detailed experimental workflow supported by a rigorous statistical approach, including the selection of mock-ups exhibiting comparable corrosion behaviour. This strategy ensures meaningful comparisons and enhances the reliability of performance evaluation. Within this framework, the originality of the study lies not only in refining Paraloid® B44-based systems as potential alternatives to traditional Incralac and more recent eco-friendly solutions, but also in establishing a robust and reproducible methodology. This methodology enables the systematic assessment of coating performance under controlled application parameters on representative patinated substrates, thereby producing results of greater relevance to conservation practice.

## 2. Research aim

The present study aims to assess the influence of resin concentration on the formation and protective effectiveness of a two-layer brush-applied newly developed protective formulations on bronze mock-ups with a foundry, nitrate based, patina. A special attention is devoted to a robust and reproducible experimental framework designed to systematically investigate the role of application parameters taking into account the lower homogeneity of realistic patinated substrates with respect to coating standard testing practices.

## 3. Materials and methods

### 3.1. Substrate

Mock-ups were prepared by an artistic foundry in Milan (*Fonderia Artistica Battaglia*). The specimens consist of quaternary bronze with a composition of 88.3% Cu, 5.7% Sn, 1.6% Pb, and 3.9% Zn, and have approximate dimensions of 5 cm x 5 cm. The artistic patina *Verde Messina* (Supplementary Material- Table 1s) was selected as a practice-oriented substrate, as already mentioned . The patina process involves using copper nitrate as a base layer, followed by ammonium sulphide, and effectively replicates a highly reactive surface [3,4].

### 3.2. Coatings

The coatings prepared and analysed in this research were formulated according to the recipe reported in previous work [24]. They are based on Paraloid® B44 (ethyl acrylate/methyl methacrylate copolymer) with either 5% w/w 5-mercapto-1-pheniltetrazole (MPT) or 2-amino-5-ethyl-1,3,4-thiadiazol- (AEDTA) corrosion inhibitor and 3% w/w Tinuvin® 312 (ethandiamide N'-(2-ethoxyphenyl)-N-(2-ethylphenyl)oxamide) UV stabiliser. Paraloid® B44 was purchased from Sinopia s.a.s., MPT from Alfa Aesar;

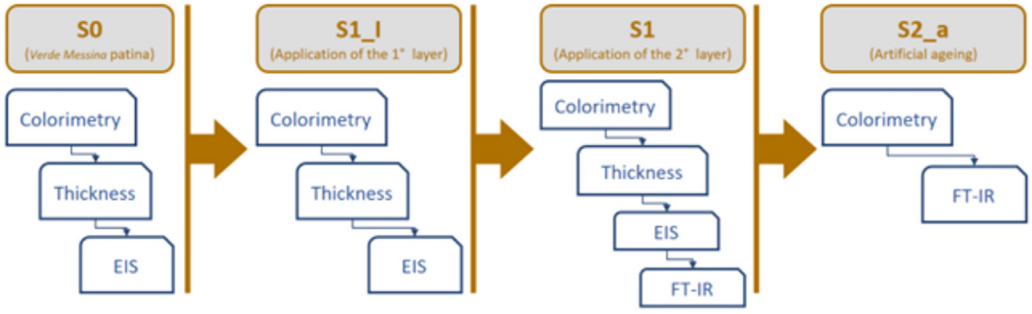


**Fig. 1.** Workflow diagram of the measurements.

AEDTA from Sigma Aldrich and Tinuvin® 312 from BASF. The solvent used to solubilize the various components and prepare the coatings was 1-methoxypropan-2-ol purchased from Sigma Aldrich.

The brush application method was chosen because it is widely adopted in conservation practices. The formulations were applied in two crisscrossed layers one week apart, in accordance with the studies of Molina et al. [14]. To investigate the possible role of Paraloid® B44 concentration in the solution, the covering capability of two layers of coating from a 10% w/w Paraloid® solution was compared with that of a layer of 5% w/w Paraloid® solution, followed by a 10% w/w top coat. Regardless of the concentration of Paraloid ® B44 in solution, the concentration of corrosion inhibitors was kept constant (Table 2s-Supplementary Material). While a concentrated solution may lead to a thicker protective film, with a higher barrier effect, a more diluted one may penetrate better and improve adhesion to the patinated substrate. The solutions were prepared by adding the various components in the following order: acrylic resin, additives, and then the solvent. They were stirred for 24 h until complete solubilisation and were applied by brush in crisscrossed layers on bronze-patinated coupons.

Each layer was left to dry in a ventilated environment (24.6 ± 3°C and 38.2 ± 5% RH) for 1 week before applying the next layer. The choice of the application method was based on the work by Molina et al. [14], with the two layers applied perpendicularly to minimize potential defects and obtain a visually uniform coating. Additionally, to ensure proper timing between layers, Molina et al. recommend waiting one week between each layer to avoid redissolution of the first layer.

### 3.3. Characterisation techniques

Surface characterisation analyses were performed as shown in Fig. 1, on patinated mock-ups without coating (S0), one week after the application of the first coating layer (S1_I), and one week after the application of the second layer (S1). A five-point measurement grid was defined with a measurement mask to achieve a more precise repositioning of instruments to monitor the evolution from S0 to S1 (Fig. 1s-Supplementary Material).

#### 3.3.1. Electrochemical impedance spectroscopy (EIS)

The corrosion behaviour of both patinated and coated coupons was evaluated by electrochemical impedance spectroscopy (EIS) using the G-PE cell developed for electrochemical analysis in metallic heritage [31]. An AISI 316 stainless steel wire (1.5 mm thick) and AISI 316 stainless steel mesh were used as pseudo reference and counter electrodes, respectively. The gel inside the cell is composed of 2% of agarose in an electrolyte solution that simulates rain according to the study of Timoncini et al. [32].

The measurement was performed in the central area of mock-ups (point E) with a Gamry Reference 600 potentiostat in five steps: 1) OCP (open Circuit Potential) measurement for 30 min, to let the system to stabilise 2) linear polarisation resistance (LPR) measurement from −10 mV to 10 mV around Eoc with a scan rate of 0.1667 mV/sec; 3) OCP measurement for 16 min; 4) EIS measurement from 100 kHz to 10 mHz with Vrms=10 mV and 10 points/decade; 5) OCP measurement for 5 min. The mock-up area exposed to the electrolyte was 3.14 $cm^2$. Gamry EchemAnalyst software was used to obtain polarisation resistance Rp from LPR measurements. The EIS spectra were represented as Bode plots (i.e. the impedance modulus $|Z|$, phase shift $\Phi$ vs. frequency) and Nyquist plots (the real part of impedance Zre vs the imaginary part Zi). The plots were used to quickly assess similarities and differences among the spectra measured on patinated mock-ups without coating (S0). The interpretation of EIS results for coated mock-ups (S1) was performed in a simplified way, based on the value of the impedance modulus at low frequency (10 mHz). For typical EIS spectra of coating, it has been shown that this value is a good approximation for the Polarisation Resistance Rp, which provides a characterisation of the protective efficacy of the coating [14]; the larger the Rp, the lower is the corrosion rate.

#### 3.3.2. Thickness measurements

Thickness measurements of the patinated and coated mock-ups were carried out with an Elcometer 456, using a probe for non-ferrous materials based on eddy currents. The manufacturer reports a ± 2.5 $\mu$m precision in measurement for this probe. A 12.3-micron gauge (Ser. N. KC8913) was used for calibration. Measurements were acquired on each mock-up at the five points of the measurement mask (Fig. 1s- Supplementary Material) and the average values were calculated.

#### 3.3.3. Colorimetric measurements

Colorimetric data were acquired using the portable spectrophotometer CM-700d Konica Minolta, in reflectance mode, with the specular component included (SCI) and excluded (SCE), using a measurement area (MAV) of 8 mm diameter, a measurement range of 360–700 nm, under D65 illuminant and a 10° observer. Three measurements were acquired on each mock-up at the three points a-e-d arranged on the diagonal of the measurement mask CIE L*, a*, and b* colour variables were used, and colour differences were calculated according to the CIE76 formula:

$$\Delta E * ab \sqrt{(\Delta a^*)^2 + (\Delta b^*)^2 + (\Delta L^*)^2} \quad (1)$$

For each mock up, colour coordinates L*, a* and b* were acquired for a total of 9 measurements (3 sites of measure, 3 measurements for each site) then the average values were calculated.

#### 3.3.4. Fourier-transformed infrared spectroscopy

Possible chemical changes of the coatings were evaluated by FTIR in external reflection mode. A Bruker Alpha II spectrometer operating in external reflection mode (ER-FTIR) was used, collecting 128 scans with a resolution of 4 $cm^{-1}$ in the range from

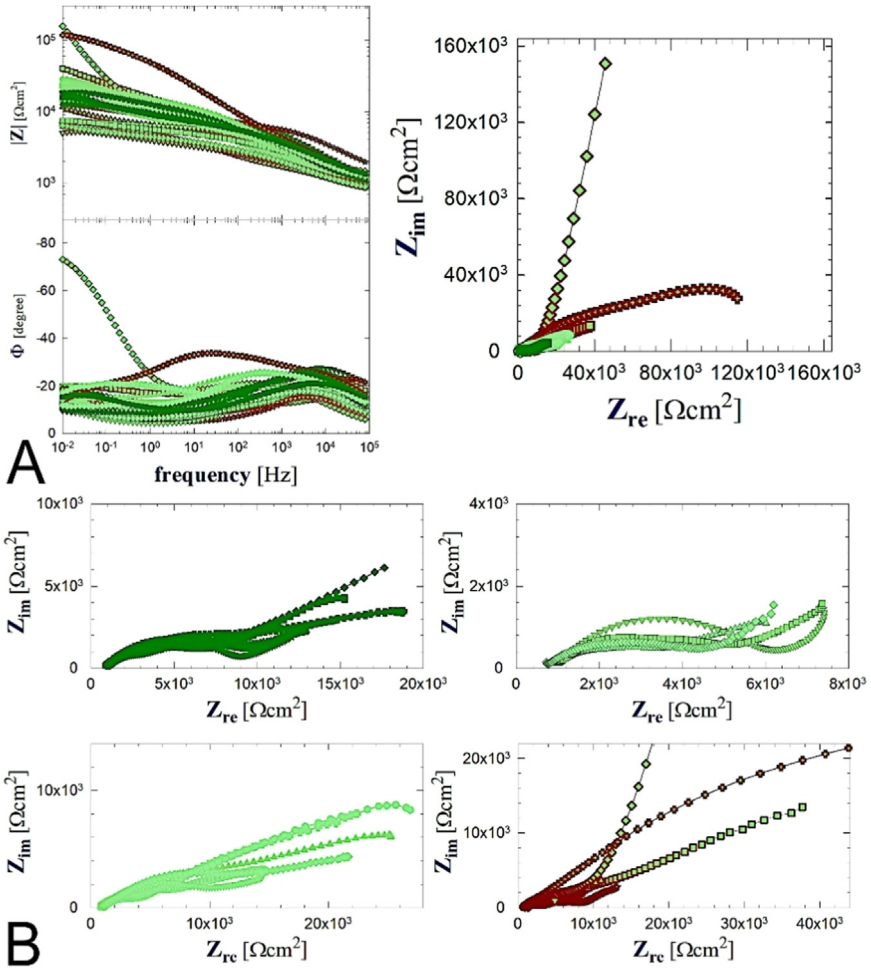


**Fig. 2.** EIS spectra on the 24 mock-ups with Verde Messina patina a) Bode and Nyquist plots; b) Nyquist plot for groups of similar spectra; the last one (red lines) groups the more peculiar spectra.".

7500 cm-1 to 375 $cm^{-1}$. Spot size was 5 mm in diameter at the centre of the mock up (point E). Spectra were represented using the pseudo absorbance [A' = log(1/R); R = reflectance] as the intensity unit. Measurements were done on the central area of fully coated mock-ups (S1) and after artificial ageing (S2).

### 3.4. Artificial ageing

The coated coupons were placed in an Angelantoni Challenge 500 climate chamber to simulate an accelerated thermo-hygrometric ageing process using thermo-hygrometric cycles, with temperature and relative humidity settings configured as indicated in Table 3s-Supplementary Material.

Each thermo-hygrometric cycle lasts approximately 6 h, allowing for 4 cycles to be completed per day. After 60 cycles (15 days), the coupons were removed from the climate chamber and subjected to a series of inspections to assess the presence of any chromatic, morphological, and/or compositional variations in the patinas and coatings.

### 3.5. Principal component analysis (PCA)

Data treatment was carried out using PLS Toolbox version 9.2.1 running on Matlab environment (version R2023b).

PCA was applied to FTIR data. The studied range was 1450–5500 $cm^{-1}$. Baseline correction (WLS algorithm), Smoothing (19 pt window, tails weighted), SNV and Mean Center pretreatments were applied to this dataset as implemented in the software [26,27].

## 4. Results and discussion

Firstly, the surface properties of the 24 patinated mock-ups used to test the application of the coatings were characterised. Fig. 2a shows Bode and Nyquist plots for the EIS measurements on each coupon. The marked variability observed among the EIS spectra of the samples highlights the complex heterogeneity of these foundry-patinated mock-ups, where differences in patina thickness and the irregular distribution of pores strongly influence the electrochemical behaviour. These curves provide valuable insights into the diverse patina behaviours, and similarities in their shapes can be linked to comparable patina morphologies. EIS spectra proved to be a powerful tool for identifying and excluding mock-ups with peculiar behaviour, which would have been unsuitable for assessing the effectiveness of the application method (Fig. 2, red plots). Moreover, the technique enabled systematic grouping of the remaining mock-ups based on the shape and range of their EIS curves, highlighting its ability to classify samples and guide rational further analysis (Fig. 2b, green plots).

The selected 16 mock-ups were evenly distributed into four equivalent sets characterised by almost the same average thickness, colour, and polarisation resistance values of the measured parameters (Table 1). Although triplicate coupons are typically used in corrosion studies, four coupons were assigned to each set to better

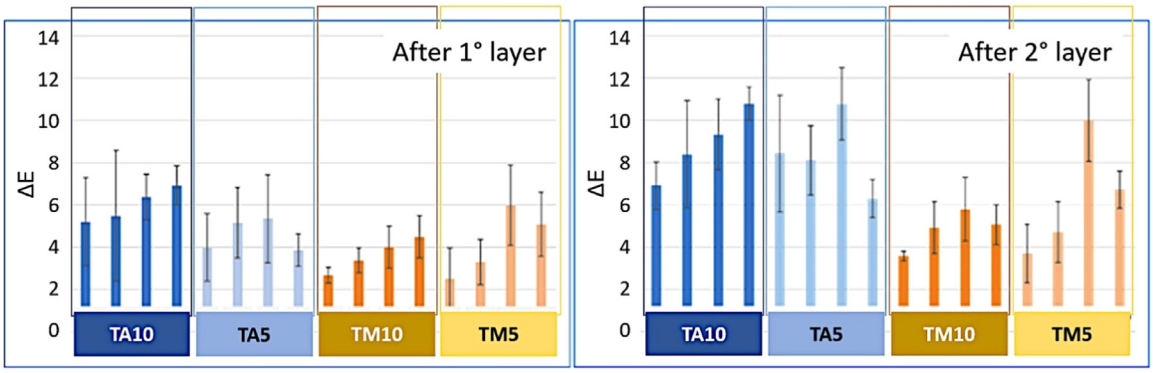


**Fig. 3.** ΔE* after the application of the first coating layer (left) and the second layer (right) on each of the four mock-ups coated with the treatments listed in Table 2s-Supplementary Material.

**Table 1**
Average values and standard deviation of thickness, colour and EIS measurements of the four sets of mock-ups at S0 (bare patina).

| S0 - Patina | | | | |
|---|---|---|---|---|
| thickness | colour | | | EIS |
| **59 ± 12** | **67 ± 2** | **-19 ± 3** | **1 ± 2** | **18 ± 8** |
| s [mm] | L* | a* | b* | <Rp> [KΩ cm$^2$] |
| 59 ± 13 | 68 ± 1 | -18 ± 2 | 2 ± 1 | 21 ± 10 |
| 59 ± 16 | 67 ± 2 | -20 ± 4 | 2 ± 3 | 19 ± 11 |
| 59 ± 14 | 67 ± 2 | -20 ± 3 | 0 ± 2 | 15 ± 6 |
| 59 ± 6 | 66 ± 2 | -19 ± 1 | 2 ± 1 | 17 ± 6 |

cope with the large variability of the surface properties of these patinated mock-ups.

Each set was then randomly assigned to one of the treatment methods described in Table 2 and coatings were applied as described in the Materials and Methods section. In addition to providing an overview of all the characterisation results, Table 2 also shows the evolution of the key properties from the bare patina (S0) to the double-layer coating (S1).

Colourimetric measurements were used to characterise the visual appearance and explore which colour coordinate has the greatest impact on the overall colour change. The colour changes ΔE* after the application of the first and second coating layers are shown in Fig. 3. Both after applying the first and the second layer, AEDTA treatments (TA10, TA5) produce more noticeable changes in the L* and b* colour coordinates than MPT treatments (TM10, TM5). This indicates a darkening (reduction of L* coordinate) and a yellowing of the surface (increase of the b* coordinate). Even so, these values are still considered acceptable for patinated bronze surfaces [28]. This was also visible to the naked eye, with a darkening of the surface (Supplementary material, Fig. 3s,4s,5s,6s).

Moreover, the glossy appearance typically observed in Incralac coatings [6,7] was not visually evident. Regarding the concentration of Paraloid in the formulation, it can be seen that, in all cases, the colour difference increases when a second layer of treatment is applied. However, despite the high standard deviations and some anomalous mock-ups, there appears to be a tendency towards less colour change in coatings made from 5% w/w solutions (i.e. TA5 and TM5).

The thickness measurements (Fig. 2s Supplementary Material, Tables 1 and 2) were used to determine whether Paraloid® concentration in the different formulations could affect the overall thickness. The instrument probe shows limitations for this type of uneven, porous surface, leading to significant variability in the data due to the high roughness of the patina (Ra=10±3 μm [29]) relative to the probe area. Nevertheless, this technique could still provide a rough estimate of the patina thickness [23]. The results indicate that after applying the first coating layer (S1_I), the measured thickness remains almost the same or decreases: this may be due to a balance between, the brush removing small, incoherent patina particles, and a first layer that may have penetrated and partially filled the surface porosity. The large measurement uncertainty do not allow to clearly identify a correlation with inhibitor used or Paraloid concentration. The average thickness of the second layer (S1) is higher than that of the bare patina. Thickness differences between S0 and S1, ranging from 1 to 6 μm, were measured, which are near the instrument detection limit. However, the results indicate that all the application methods yield coatings with similar thicknesses, allowing comparison of their corrosion protection via electrochemical analyses.

Tables 1 and 2 and Fig. 4 summarise the Rp average values obtained from LPR and EIS measurements for each coupon on bare patina and after the first and the second coating layer. The mock-ups with bare patina are characterised by an Rp around 18 KΩcm$^2$, in the range of the value reported for similar patinas [3], suggesting they do not protect the bronze substrate and highlighting the need to develop optimal procedures for preserving this surface finish. The coupons treated with AEDTA coatings (TA) show two orders of magnitude higher corrosion resistance than bare patina after the second layer is applied, with no significant difference between TA10 (treatment with two layers of Paraloid 10% w/w) and TA5 (treatment with the first layer with 5% w/w of Paraloid and the second layer with Paraloid 10% w/w). In contrast, coupons treated with MPT coatings exhibit slightly lower Rp values, indicating reduced protective effectiveness.

It is worth noting that the widespread results obtained on the rough, porous foundry-patinated mock-ups we adopted for this study are consistent with the complex surface texture of bronze artworks. Nonetheless, an overall trend can be identified across the four mock-up groups with different protective treatments. Bode plots (Fig. 5) further clarify the evolution of the impedance response. They clearly show a greater increase in corrosion resistance after applying the second layer in all cases. This is particularly

**Table 2**
Average values and standard deviation of thickness, colour and EIS measurements the four sets of mock-ups after the first layer (S1_I) and the second layer (S1) of the selected treatment (TA: formulation with AEDTA, TM: formulation with MPT. TA10, TM10: both layers with 10% w/w Paraloid in solvent; TA5, TM5; first layer 5% w/w and second layer 10% w/w Paraloid in solvent).

| | S1_I - Coating first layer | | | | | S1 - Coating (double layer) | | | | | |
|---|---|---|---|---|---|---|---|---|---|---|---|
| | thickness | colour | | | EIS | thickness | colour | | | EIS | |
| treatment | s [μm] | L* | a* | b* | <$R_p$> [MΩ cm$^2$] | s [μm] | L* | a* | b* | <$R_p$> [MΩ cm$^2$] | <ΔE*> |
| TA10 | 56 ± 18 | 62 ± 1 | -19 ± 2 | 3 ± 1 | 0,8 ± 0,7 | 60 ± 20 | 60 ± 1 | -20 ± 2 | 5 ± 1 | 4 ± 3 | 9 ± 2 |
| TA5 | 65 ± 15 | 63 ± 3 | -21 ± 5 | 4 ± 3 | 0,25 ± 0,09 | 74 ± 9 | 60 ± 4 | -21 ± 5 | 6 ± 2 | 3 ± 2 | 8 ± 2 |
| TM10 | 57 ± 13 | 64 ± 2 | -21 ± 3 | 1 ± 2 | 0,5 ± 0,4 | 66 ± 17 | 62 ± 3 | -21 ± 3 | 2 ± 2 | 2 ± 2 | 5 ± 1 |
| TM5 | 55 ± 6 | 63 ± 2 | -20 ± 1 | 3 ± 1 | 0,4 ± 0,3 | 64 ± 13 | 60 ± 2 | -19,9 ± 0,5 | 3 ± 1 | 0,7 ± 0,2 | 6 ± 3 |

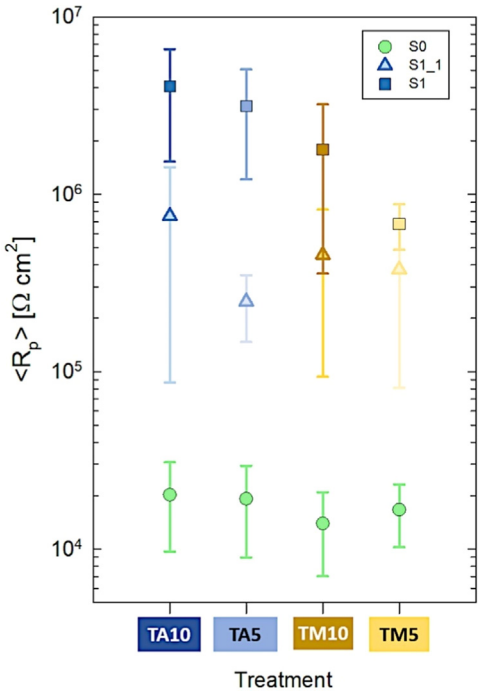


**Fig. 4.** Average polarisation resistance values on bare patina (circle), after the application of the first coating layer (square) and the second layer (diamond) on each of the four mock-ups coated with the treatments listed in Table 2s-Supplementary Material.

evident in the AEDTA-containing treatments, which highlights the role of resin concentration. After applying the first layer, consisting of a more diluted formulation (Paraloid 5% w/w), |Z| values are nearly one order of magnitude lower than those measured for the more concentrated formulation (Paraloid 10% w/w). However, similar |Z| values are achieved when the second layer is finally applied.

Based on these results, AEDTA appears to be a more effective corrosion inhibitor than MPT on *Verde Messina* patinated bronze surfaces. It provides superior corrosion protection and, as observed in previous studies [24], it is more stable over time. Therefore, TA5 is the most suitable application method, as it provides comparable corrosion protection while requiring less acrylic resin. In addition, TA5 exhibits an enhanced ability to penetrate the pores of the mock-up surfaces, thereby promoting superior adhesion and overall coating performance.

Finally, the behaviour of the coatings applied to patinated mock-ups and subjected to thermo-hygrometric ageing was examined. The photooxidative stability of these same coatings was investigated in a previous study [24] by exposure to artificial sunlight. That study, showed that coatings based on Paraloid® B44, AEDTA and Tinuvin® 312 are the most resistant to photo-oxidative degradation, and also that they are capable of retaining the corrosion inhibitor for longer, thereby slowing its release into the environment. However, the effect of temperature and humidity on the performance of the coatings was not taken into account. To address this issue, thermo-hygrometric ageing has been carried out for the treatment application on the patinated mock-ups of this study.

After the thermo-hygrometric ageing, no visible changes were observed. The colour change ($\Delta E^*$) before and after artificial ageing of all coatings is below the threshold of perceptibility for the human eye ($\Delta E^*$=3 [30]), as shown in Fig. 6. Coatings containing AEDTA showed slightly higher $\Delta E$ values, mainly due to an increase in the b* coordinate. The average $\Delta E$ is approximately 2 for TA10 and TA5, while it is about 1 for TM10 and TM5.

A comparison of the FTIR spectra of all the coated coupons before and after ageing showed no significant differences. This suggests that no detectable molecular changes occurred, confirming the chemical stability of the treatments during the initial stages of the thermo-hygrometric ageing. These results support the potential suitability of the tested formulations for the long-term protection of outdoor bronze surfaces. Fig. 7 compares representative FTIR spectra of the unaged (S1) and aged (S2) coatings for each type of treatment and application method. These spectra were selected as representative examples for each coupon set because they reflect the overall spectral trends observed across the replicates. The characteristic absorption bands - such as those assigned to the $\nu$ C=O vibration of the acrylic resin (~1730 cm$^{-1}$), $\nu$ CH stretching (~2950–2850 cm$^{-1}$), $\delta$ CH bending (1450–1385 cm$^{-1}$) and ester group vibrations (~1250–1150 cm$^{-1}$) - remain unchanged in in-

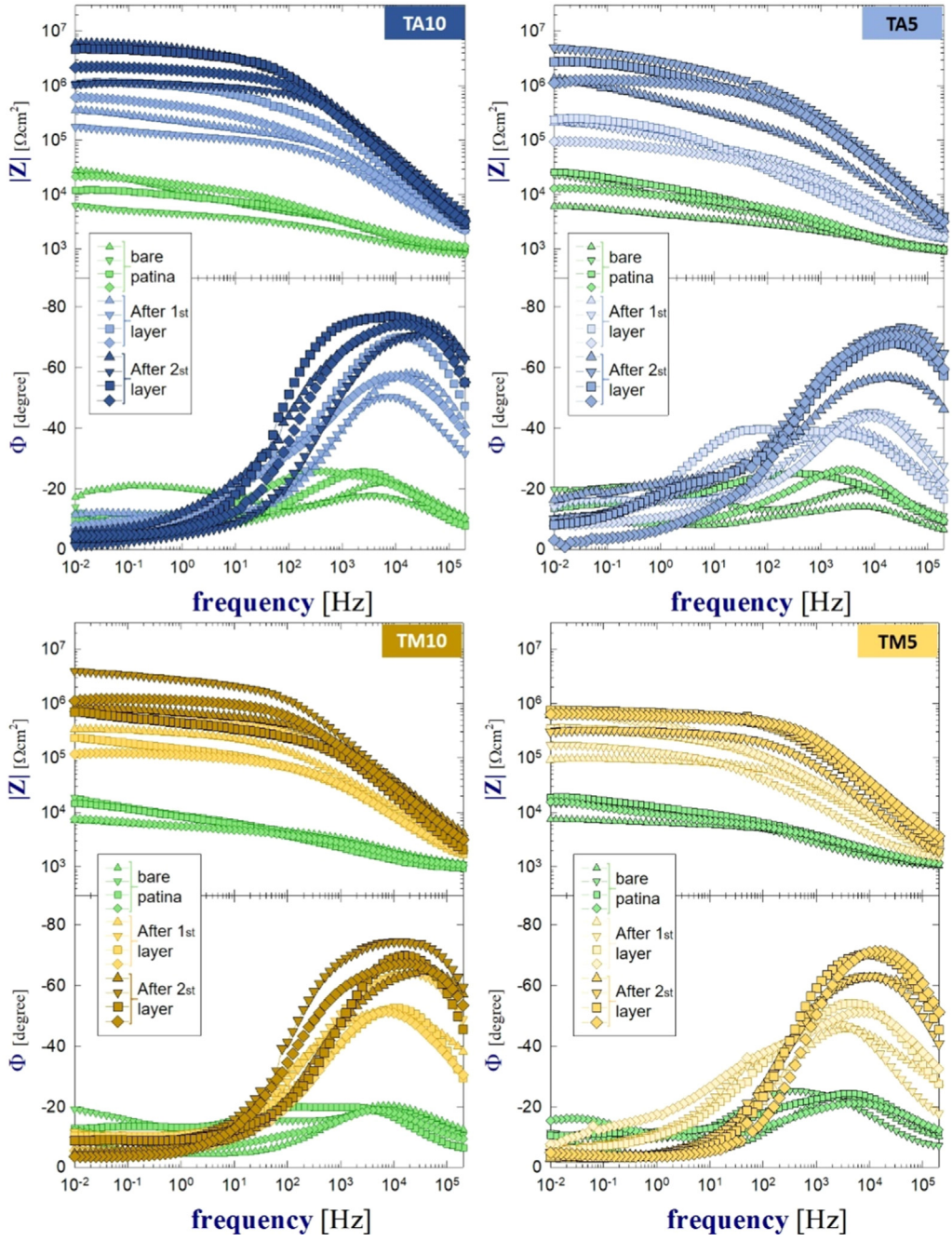


**Fig. 5.** EIS Bode plots of the mock-ups with bare patina (green), and after the application of the first (lighter colour) and second (darker colour) coating layer according to the treatments listed in Table 2s-Supplementary Material.

tensity and position after ageing [33,34]. This further confirms the preservation of the chemical structure of the coating. In addition to the absorption bands associated with the acrylic coating, some vibrations attributable to the underlying basic copper nitrate patina (polymorphs gerhardtite and rouaite, $Cu_2(NO_3)(OH)_3$) [3] are also visible in the spectra. These include bands assigned to either structural or hydrogen-bonded OH groups (3544 and 3427 $cm^{-1}$, respectively), overtone or combination transitions of fundamental vibrational modes between 2800 and 2000 $cm^{-1}$, and the $\nu$ N–O vibration of a monodentate O–NO group at 1045 $cm^{-1}$, and the $\nu$ Cu-O at 504 $cm^{-1}$ [35,36]. Such bands remain stable over time and further support the protective efficacy of the treatments. Additionally, the spectral profiles remain consistent across different concentrations of Paraloid B44, indicating that the chemical properties of the coating are not significantly affected by the adopted %w/w variations.

Although only subtle variations could be discerned in the qualitative comparison of the FTIR spectra, Principal Component Analysis (PCA) was employed to determine whether these minor differences corresponded to meaningful chemical variations among the treatments. Chemometric analysis proved to be a valuable approach for enhancing the sensitivity of spectral interpretation, allowing us to detect subtle yet consistent changes in the coatings over time and to distinguish the contributions of individual components within the formulation during ageing. This method has previously been applied to study the degradation of the same coatings on inert supports. The present results were in agreement with traditional visual assessments, while providing a more refined per-

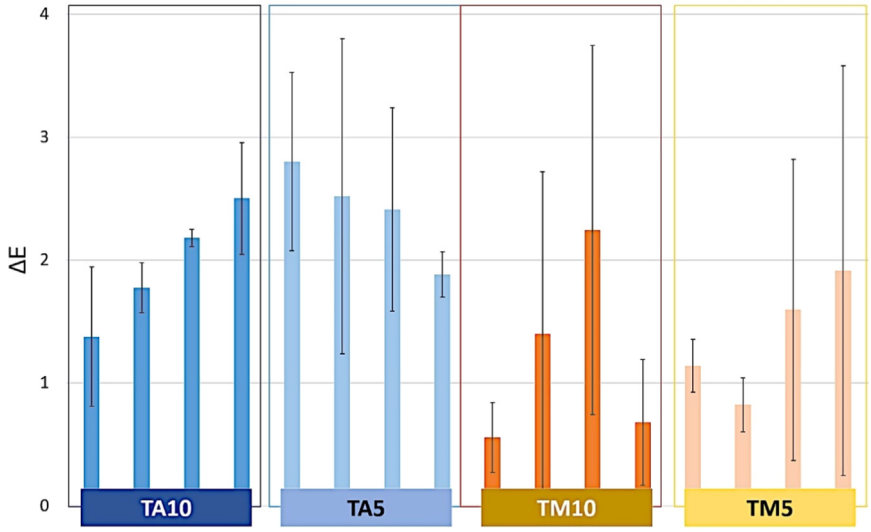


**Fig. 6.** Colour difference after artificial ageing for each coupon.

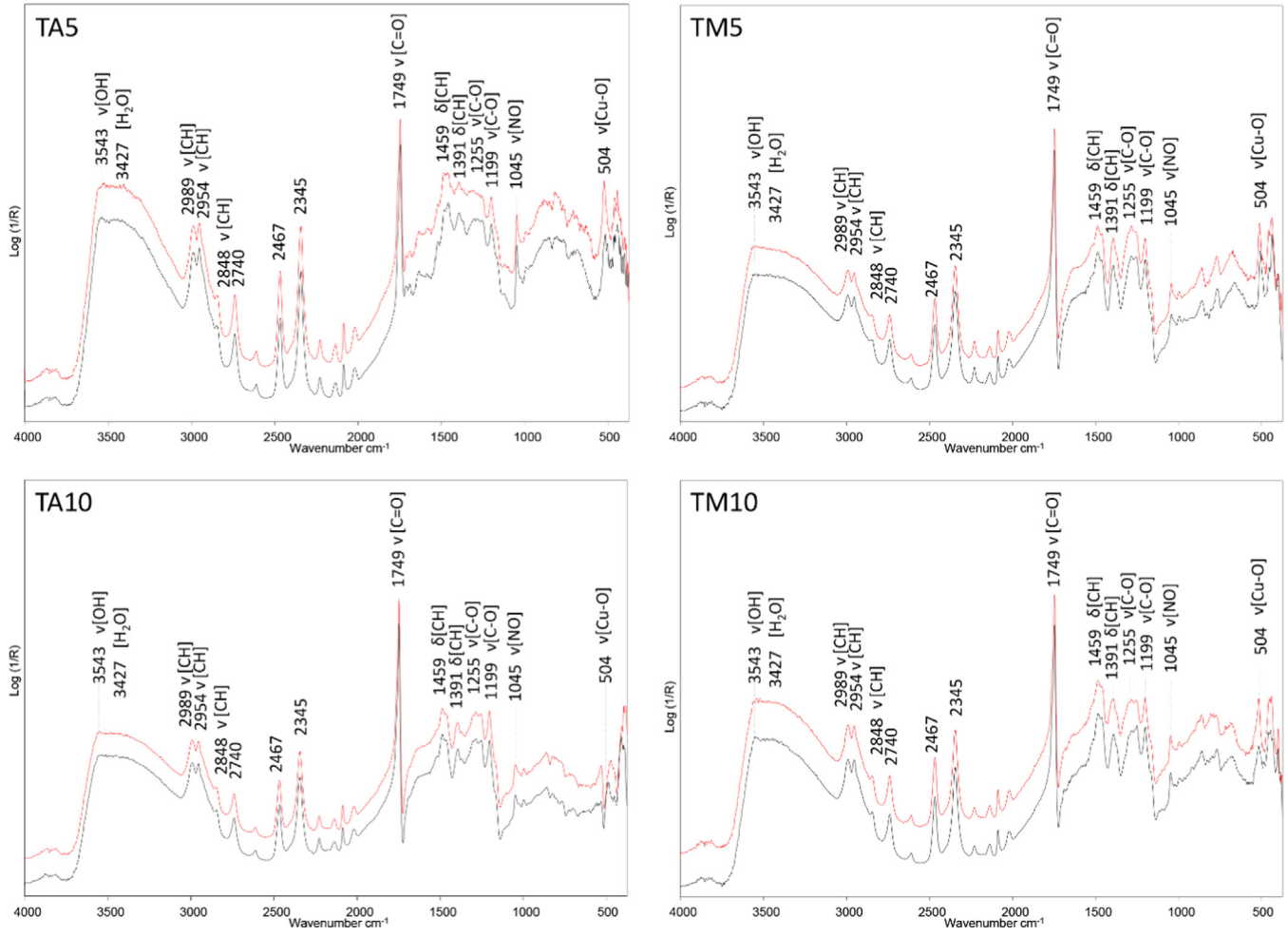


**Fig. 7.** Comparison of representative FTIR spectra of unaged (S1 - black line) and aged (S2 - red line) coated coupons for each type of treatment and application method.

spective on the decay processes and the differentiation among the various formulations [26]. Fig. 8 shows the score plot of the first principal component versus the second principal component for the tested specimens, with colours indicating the various treatments. The PCA results distinctly separate the treatments with the two kinds of corrosion inhibitors, as anticipated. The second principal component (PC2) primarily distinguishes the MPT samples (TM10, TM5) from the AEDTA samples (TA10, TA5), accounting for the principal source of variance. MPT samples occupy a larger area in the PCA space than AEDTA samples, highlighting greater variability within this group. Furthermore, the MPT samples are more widely dispersed, indicating more significant differences between

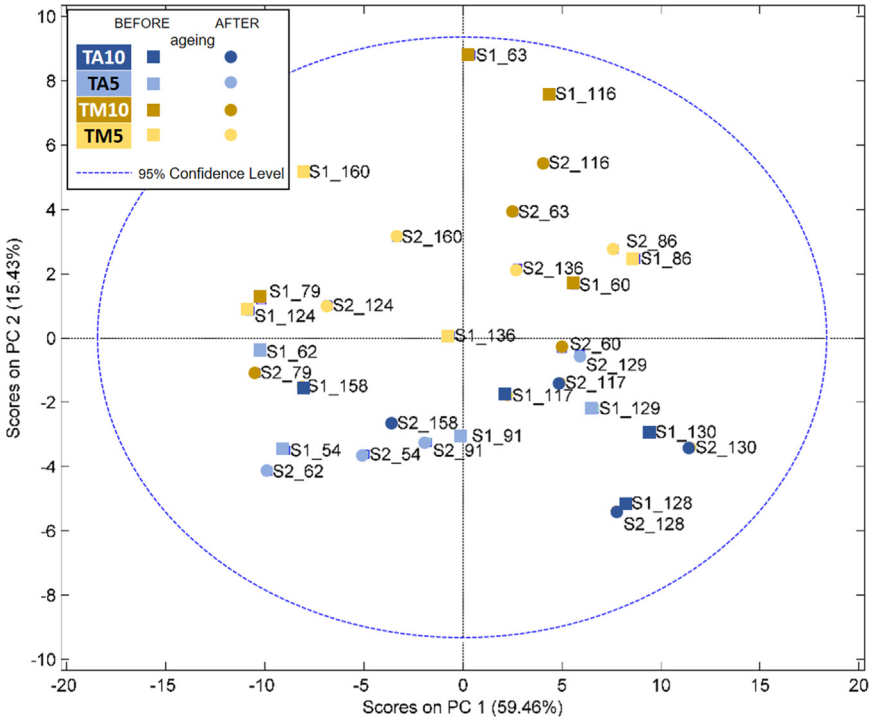


**Fig. 8.** PCA results of the artificially aged coupons.

the "before" and "after" ageing conditions. In contrast, the AEDTA samples with a double layer of Paraloid 10% w/w (TA10) cover a slightly broader area than the AEDTA samples with the more diluted first layer (TA5), making the TA5 group the most compact. This compactness suggests the smallest changes over time, which aligns precisely with the stability we seek to identify.

## 5. Conclusions

This study investigates the application of Paraloid® B44-based coatings to bronze mock-ups with a highly reactive foundry patina (*Verde Messina*). We examined coatings formulated with 5% w/w of either AEDTA or MPT, two sustainable corrosion inhibitors, focusing on the role of Paraloid® concentration in a two-layer brush application. The intrinsic variability of the foundry-patinated substrates, representative of the surfaces of real bronze artworks, was elucidated using non-destructive analytical techniques, and the importance of carefully selecting comparable mock-up groups for reliable performance assessment is highlighted. Colourimetry, coating thickness measurements, and Electrochemical Impedance Spectroscopy (EIS) were used jointly to characterise the aesthetic and physicochemical surface properties and their evolution under protective treatments. The foundry patina exhibited an average polarisation resistance of approximately 18 kΩ·cm², indicating limited protective capability. All coating systems significantly improved their corrosion resistance. In particular, AEDTA-based treatments (TA10 and TA5) increased Rp values of about two orders of magnitude (2–4 MΩ·cm²). MPT-based systems showed lower Rp values, confirming their reduced protective effectiveness. Aesthetically, all treatments induced moderate colour variations, with $\Delta E^*$ values ranging from 5 to 9 after application, mainly due to decreases in $L^*$ and increases in $b^*$, but remaining within acceptable visual thresholds. Thickness measurements showed minimal differences between treatments, with variations between coated and uncoated samples ranging from 1 to 6 µm, confirming comparable film formation across all application methods. Notably, no significant differences in protective performance were observed between the two application approaches: two consecutive layers of 10% w/w Paraloid® or a sequential application of 5% followed by 10% w/w solutions. Thermo-hygrometric ageing yielded preliminary conclusions about the overall stability of all coatings, with a $\Delta E$ of approximately 1–2, which remains below the perceptibility threshold ($\Delta E = 3$), indicating good visual stability and no chemical changes detected by FTIR. However, multivariate analysis (PCA) highlighted greater stability in systems with the first layer containing a 5% w/w Paraloid® solution. Among the systems tested, TA5 emerged as the preferred treatment, as its performance is comparable to TA10 while using a smaller amount of Paraloid®. The adopted methodology allowed for the analytical characterisation of the influence of the application method on a thick and rough patinated surface similar to that of works of art.

Future research will aim to validate these results under more complex conditions, particularly outdoor weathering in an urban marine environment, to assess the long-term performance and durability of the coatings.

## Funding sources

This research was funded by Progetto di Ricerca di Interesse Nazionale PRIN 2022 “Innovative multi analytical Characterisation of the influence of pAtina-coating inteRaction on anti-corrosive propErties – InCARE” (Project code: 2022895PTX), funded by MUR and the European Union – Next Generation EU, M4.C2.1.1, CUP B53D23001230006.

## Supplementary materials

Supplementary material associated with this article can be found, in the online version, at doi:10.1016/j.culher.2026.04.016.

## References

[1] E. Bernardi, C. Chiavari, B. Lenza, C. Martini, L. Morselli, F. Ospitali, L. Robbiola, The atmospheric corrosion of quaternary bronzes: the leaching action of acid rain, Corros. Sci. 51 (2009) 159–170, doi:10.1016/j.corsci.2008.10.008.

[2] L. Robbiola, C. Fiaud, S. Pennec, New model of outdoor bronze corrosion and its implications for conservation, in: ICOM Committee for Conservation Tenth Triennial Meeting, Washington DC, United States, 1993, pp. 796–802. https://hal.science/hal-00975704v1.
[3] C. Petiti, L. Toniolo, L. Berti, S. Goidanich, Artistic and laboratory patinas on copper and bronze surfaces, Appl. Sci. 13 (2023), doi:10.3390/app132111873.
[4] H. Otmačić Ćurković, T. Kosec, K. Marušić, A. Legat, An electrochemical impedance study of the corrosion protection of artificially formed patinas on recent bronze, Electrochim. Acta 83 (2012) 28–39, doi:10.1016/j.electacta.2012.07.094.
[5] B. Salvadori, A. Cagnini, M. Galeotti, S. Porcinai, S. Goidanich, A. Vicenzo, C. Celi, P. Frediani, L. Rosi, M. Frediani, G. Giuntoli, L. Brambilla, R. Beltrami, S. Trasatti, Traditional and innovative protective coatings for outdoor bronze: application and performance comparison, J. Appl. Polym. Sci. 135 (2018), doi:10.1002/app.46011.
[6] J. Wolfe, R. Grayburn, A review of the development and testing of Incralac lacquer, J. Am. Inst. Conserv. 56 (2017) 225–244, doi:10.1080/01971360.2017.1362863.
[7] J. Wolfe, R. Grayburn, H. Khanjian, A. Heginbotham, A. Phenix, Deconstructing Incralac: a formulation study of acrylic coatings for the protection of outdoor bronze sculpture, ICOM-CC 18th Triennal Conference, 2017.
[8] E. Cano, D. Lafuente, Corrosion inhibitors for the preservation of metallic heritage artefacts, in: Corrosion and Conservation of Cultural Heritage Metallic Artefacts, Elsevier Ltd, 2013, pp. 570–594, doi:10.1533/9781782421573.5.570.
[9] A. Balbo, C. Chiavari, C. Martini, C. Monticelli, Effectiveness of corrosion inhibitor films for the conservation of bronzes and gilded bronzes, Corros. Sci. 59 (2012) 204–212, doi:10.1016/j.corsci.2012.03.003.
[10] M.T. Molina, E. Cano, B. Ramírez-Barat, Protective coatings for metallic heritage conservation: a review, J. Cult. Herit. 62 (2023) 99–113, doi:10.1016/j.culher.2023.05.019.
[11] M.P. Casaletto, V. Figà, A. Privitera, A. Mazzaglia, A. Scala, R. Zagami, Sustainable corrosion inhibition of copper-based alloys by smart $\beta$-cyclodextrin/benzotriazole complexes, in: Proceedings of the 5th European Cyclodextrin Conference, Lisbon, Portugal, 2017, pp. 3–6.
[12] M.P. Casaletto, C. Cirrincione, A. Privitera, V. Basilissi, A sustainable approach to the conservation of bronze artworks by smart nanostructured coatings, in: Metal 2016, Proceedings of the Interim Meeting of the ICOM-CC Metal Working Group, Paris, France, International Council of Museums, 2016, pp. 144–152.
[13] I. Eliboev, E. Berdimurodov, K. Yakhshinorov, J. Abdisattarov, O. Dagdag, A. Berisha, W.B. Wan Nik, A. Kholikov, K. Akbarov, Supramolecular corrosion protection: ecofriendly synthesis and efficacy of a $\beta$-cyclodextrin/o-phenylenediamine complex, J. Taiwan. Inst. Chem. Eng. 147 (2023), doi:10.1016/j.jtice.2023.104944.
[14] M.T. Molina, E. Cano, B. Ramírez-Barat, Testing protective coatings for metal conservation: the influence of the application method, Herit. Sci. 11 (2023), doi:10.1186/s40494-023-00937-0.
[15] G. Masi, J. Esvan, C. Josse, C. Chiavari, E. Bernardi, C. Martini, M.C. Bignozzi, N. Gartner, T. Kosec, L. Robbiola, Characterization of typical patinas simulating bronze corrosion in outdoor conditions, Mater. Chem. Phys. 200 (2017) 308–321, doi:10.1016/j.matchemphys.2017.07.091.
[16] T.E. Graedel, K. Nassau, J.P. Franey, Copper patinas formed in the atmosphere—I. Introduction, Corros. Sci. 27 (1987) 639–657, doi:10.1016/0010-938X(87)90047-3.
[17] L. Robbiola, J.M. Blengino, C. Fiaud, Morphology and mechanisms of formation of natural patinas on archaeological Cu–Sn alloys, Corros. Sci. 40 (12) (1998) 2083–2111, doi:10.1016/S0010-938X(98)00096-1.
[18] L. Selwyn, Metals and Corrosion: A Handbook for the Conservation Professional, Canadian Conservation Institute, Ottawa, 2004.
[19] T. Kosec, M. Leban, P. Ropret, M. Finšgar, The impact of urban rain on the changes of bare and artificially patinated bronze during 9-year exposure, Environ. Sci. Pollut. Res. Int. 31 (2024) 31925–31941, doi:10.1007/s11356-024-33369-9.
[20] G. Di Carlo, C. Giuliani, C. Riccucci, M. Pascucci, E. Messina, G. Fierro, M. Lavorgna, G.M. Ingo, Artificial patina formation onto copper-based alloys: chloride and sulphate induced corrosion processes, Appl. Surf. Sci. 421 (2017) 120–127, doi:10.1016/j.apsusc.2017.01.080.
[21] V. Hayez, T. Segato, A. Hubin, H. Terryn, Study of copper nitrate-based patinas, J. Raman Spectrosc. 37 (2006) 1211–1220, doi:10.1002/jrs.1591.
[22] D.A. Scott, Copper and Bronze in Art: Corrosion, Colorants, Conservation, Getty Conservation Institute, 2002.
[23] P. Letardi, Testing new coatings for outdoor bronze monuments: a methodological overview, Coatings 11 (2021), doi:10.3390/coatings11020131.
[24] G. Pellis, B. Giussani, P. Letardi, T. Poli, P. Rizzi, B. Salvadori, A. Sansonetti, D. Scalarone, Improvement in the sustainability and stability of acrylic protective coatings for outdoor bronze artworks, Polym. Degrad. Stab. 218 (2023), doi:10.1016/j.polymdegradstab.2023.110575.
[25] G. Pellis, F. Caldera, F. Trotta, T. Biazioli de Oliveira, P. Rizzi, T. Poli, D. Scalarone, Enhancing permanence of corrosion inhibitors within acrylic protective coatings for outdoor bronze using green nanocontainers, Molecules 29 (2024), doi:10.3390/molecules29235702.
[26] G. Pellis, M. Tiburziano, B. Giussani, P. Letardi, B. Salvadori, A. Sansonetti, D. Scalarone, Advancing preservation: a chemometric approach for monitoring the degradation of protective coatings for bronze statues, Microchem. J. 210 (2025) 112971, doi:10.1016/j.microc.2025.112971.
[27] J. Riu, B. Giussani, Analytical chemistry meets art: the transformative role of chemometrics in cultural heritage preservation, Chemom. Intell. Lab. Syst. 247 (2024) 105095, doi:10.1016/j.chemolab.2024.105095.
[28] L.B. Brostoff, Coating Strategies for the Protection of Outdoor Bronze Art and Ornamentation, Universiteit van Amsterdam Amsterdam, Netherlands, 2003.
[29] G. Pellis, C. Biondi, M. Tiburziano, B. Giussani, P. Letardi, T. Poli, A. Sansonetti, B. Salvadori, P. Rizzi, D. Scalarone, InCare project: narrowing the gap between laboratory studies and conservation practice, in: N. Emmerson, J. Thunberg, D. Watkinson (Eds.), Metal 2025, 2025, pp. 155–162. https://hdl.handle.net/20.500.14243/555519.
[30] R.F. Witzel, R.W. Burnham, J.W. Onley, Threshold and suprathreshold perceptual color differences, J. Opt. Soc. Am. 63 (1973) 615–625, doi:10.1364/JOSA.63.000615.
[31] B. Ramírez Barat, E. Cano, P. Letardi, Advances in the design of a gel-cell electrochemical sensor for corrosion measurements on metallic cultural heritage, Sens. Actuators B Chem. 261 (2018) 572–580, doi:10.1016/j.snb.2018.01.180.
[32] A. Timoncini, E. Brattich, E. Bernardi, C. Chiavari, L. Tositti, Safeguarding outdoor cultural heritage materials in an ever-changing troposphere: challenges and new guidelines for artificial ageing test, J. Cult. Herit. 59 (2023) 190–201, doi:10.1016/j.culher.2022.12.003.
[33] V. Pintus, M. Schreiner, Characterization and identification of acrylic binding media: influence of UV light on the ageing process, Anal. Bioanal. Chem. 399 (2011) 2961–2976, doi:10.1007/s00216-010-4357-5.
[34] R. Wiesinger, L. Pagnin, M. Anghelone, L.M. Moretto, E.F. Orsega, M. Schreiner, Pigment and binder concentrations in modern paint samples determined by IR and Raman spectroscopy, Angew. Chem. - Int. Ed. 57 (2018) 7401–7407, doi:10.1002/anie.201713413.
[35] J. Fu, X. Liu, L. Liu, H. Meng, X. Wang, Infrared and Raman spectral analysis of the polycrystalline copper hydroxonitrates, IOP Conf. Ser. Mater. Sci. Eng. 774 (2020) 012060, doi:10.1088/1757-899X/774/1/012060.
[36] J.M. Aguirre, A. Gutiérrez, O. Giraldo, Simple route for the synthesis of copper hydroxy salts, J. Braz. Chem. Soc. 22 (2011), doi:10.1590/S0103-50532011000300019.